

DESIGN AND EXPERIMENT OF A DOUBLE LONGITUDINAL AXIAL-FLOW CORN THRESHING DEVICE FOR LARGE FEEDING CAPACITY

大喂入量双纵轴流玉米脱粒装置设计与试验

Mingrui LI^{1,3)}, Yanchun YAO^{1,2,3*)}, Yongkang ZHU^{1,3)}, Xibin LI^{1,3)}, Dong YUE¹⁾, Duanyang GENG¹⁾

¹⁾ College of Agricultural Engineering and Food Science, Shandong University of Technology, Zibo 255000, China;

²⁾ Opening Fund of National Key Laboratory of Agricultural Equipment Technology, Beijing 100083, China

³⁾ Institute of Modern Agricultural Equipment, Zibo 255000, China;

Tel: +86-15275906287; E-mail: ycyao2018@sdut.edu.cn

DOI: <https://doi.org/10.35633/inmateh-75-45>

Keywords: corn kernel harvest; double longitudinal axial flow; large feeding amount; threshing

ABSTRACT

Traditional corn threshing devices face issues of high unthreshed grain rate and high breakage rate under conditions of high feeding rates. To address this, a high-throughput double longitudinal axial flow corn threshing device was designed in this study. Based on a stress analysis of the interaction between threshing components and corn ears, an arc-shaped plate tooth structure was developed to progressively increase the squeezing force between the plate teeth and the ears. A combined threshing element, integrating arc-shaped plate teeth and round-headed nail teeth, was designed to improve threshing cleanliness and minimize grain breakage under high feed capacity conditions. The crucial parameters of the threshing cylinder were determined by theoretical analysis. Threshing bench experiments were conducted to investigate the effects of feed rate, threshing cylinder speed, and guide plate angle on the device's grain breakage rate and unthreshed grain rate. Based on the findings, the optimal parameter ranges were identified. An orthogonal test involving three factors at three levels each was conducted to determine the optimal working parameters of the device. The results indicated that the ideal conditions were a feed rate of 16 kg/s, a threshing cylinder speed of 400 r/min, and a guide plate angle of 26°. Under these parameters, the grain breakage rate was 5.02%, and the unthreshed grain rate was 0.171%. The operational performance met the actual harvesting requirements. This research could offer a reference for the design of large-feed-rate threshing devices and related harvesters.

摘要

当前传统的玉米脱粒装置在大喂入量条件下, 存在籽粒未脱净率高、破碎率高的问题, 对此本研究设计了一种大喂入量双纵轴流玉米脱粒装置。基于脱粒元件与玉米果穗的受力分析, 本研究设计了弧形板齿结构, 逐步增加板齿与果穗之间的挤搓力, 有利于脱下不同脱粒难度的玉米籽粒; 本研究设计了“弧形板齿+圆头钉齿”组合式脱粒元件, 满足了大喂入量条件下装置实现高脱净率和籽粒破碎; 通过理论分析的方法确定了脱粒滚筒的关键参数。通过台架试验研究了该装置中喂入量、滚筒转速和导流板角度对籽粒破碎率和未脱净率的影响规律, 并确定了较优参数区间。通过三因素三水平正交试验, 确定了该装置的最佳工作参数为: 喂入量为 16kg/s、滚筒转速为 400r/min、导流板角度为 26°, 此时籽粒破碎率为 5.02%, 未脱净率为 0.171%, 作业性能满足了实际收获需求。该研究可为大喂入量脱粒装置和相关收获机设计提供参考。

INTRODUCTION

Corn occupies the largest sown area among grain crops in China and ranks second globally in production (**China, 2024). Currently, the main methods of corn harvesting are ear harvesting and direct grain harvesting (Tao et al., 2019). Threshing is an essential link in the process of direct grain harvesting. The grain breakage rate and the unthreshed grain rate are important references for assessing the effect of the threshing device and exert significant influence on the threshing quality.

¹ Mingrui Li, M.S. Stud.; Yanchun Yao, Assoc.Prof.; Yongkang Zhu, M.S. Stud.; Xibin Li, M.S. Stud.; Dong Yue, M.S. Stud.; Duanyang Geng, Prof.

The current research on corn threshing devices mainly focuses on reducing the grain breakage rate, enhancing the threshed grain rate, and threshing corn with high moisture content. Scholars have introduced innovative designs by integrating threshing theory and bionic principles, including the corn thresher element resembling a chicken beak (Xinping et al., 2015), the rigid-flexible coupling bionic threshing unit (Li et al., 2021), and the thumb-type threshing element (Jiale et al., 2023) by studying corn threshing theory and applying bionic principles. To address issues like incomplete threshing in existing axial flow threshers, scholars have developed a segmented threshing device (Yuejiang et al., 2020), the combined "threshing bow teeth and movable nail teeth" thresher separation device (Youliang et al., 2022). To reduce grain breakage caused by rigid thresher elements, optimized design yields plate teeth with protrusions (Xiaopeng et al., 2003) and elastic short rasp bars as threshing elements (Duanyang et al., 2019). These structural improvements optimize impact effects during threshing. Regarding the issue of the difficulty in threshing corn with high moisture content, numerous scholars have achieved significant progress through structural enhancements and parameter optimizations (Yujie et al., 2023; Qing et al., 2024; Jinliang et al., 2024). Some researchers explored the influence of feed rate, threshing cylinder speed and other factors on the threshing effect through experiments, and constructed relevant mathematical models, which provided reference for deep understanding of the threshing mechanism and obtaining the best working parameters (Srison et al., 2016; Cujbescu et al., 2021; Vlădut N. et al., 2022; Vlădut N. et al., 2023). Some researchers have used sensors and optimized control algorithms, which in turn provide timely and effective regulation of threshing parameters to achieve better threshing results (Maertens et al., 2004; Maertens et al., 2005; Abdeen M., 2022). To improve harvesting efficiency further, grain combine harvesters are gradually evolving towards larger scales. Therefore, threshing devices that can handle larger feed rates are needed. Currently, the research mainly concentrates on threshing devices with feed rates less than 12 kg, and there is relatively scarce research on those with feed rates greater than 12 kg. Meanwhile, the traditional threshing devices, under the circumstance of large feed rates, have issues such as high grain breakage rate and high unthreshed grain rate.

In response to the above problems, this study presents the design of a double longitudinal axial-flow corn threshing device incorporating variable-height combined threshing elements consisting of arc-shaped plate teeth and round-head nail teeth, a conical drum body, and adjustable guide vanes. Through bench experiments, the influence patterns of feed rate, threshing cylinder speed, and angle of the guide plate on grain breakage rate and unthreshed grain rate were investigated. The optimal parameter combination was acquired. This provides a reference for designing the double longitudinal axial flow threshing device with a large feeding amount.

MATERIALS AND METHODS

The Overall Structure and Working Principle of the Threshing Device

The Overall Structure

The overall structure comprises a feeding inlet, threshing drum, upper cover plate, grid concave plate screens, deflector adjustment mechanism, frame, gearbox, and motor. Notably, the rotation direction of the threshing drum on both sides is reversed, as illustrated in Figure 1.

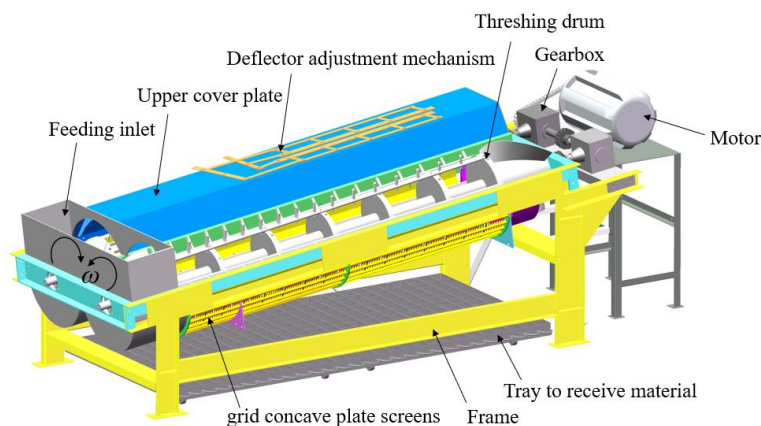


Fig. 1 - The Overall Structure of the Device

Under the harvesting condition of large feed-in volume, the double longitudinal axial-flow threshing drum has a lower rotational speed and a larger separation area than the single longitudinal axial-flow drum.

A lower rotational speed of the drum is conducive to reducing the impact force, thereby lowering the breakage of corn kernels. A larger separation area can decrease the thickness of the material layer, facilitating the timely separation of the threshed kernels out of the machine.

The Working Principle

During the threshing operation, corn ears are introduced through the feeding inlet and propelled into the threshing chamber on both sides of the double-longitudinal axial flow threshing device by the action of a screw feeding head. Under the combined influence of the threshing drum and upper cover plate, the corn ear moves toward the rear. It interacts with various components throughout this process, including threshing elements, conical drum bodies, grid concave plate screens, and striking and squeezing against other fruit ears to facilitate kernel separation from their cobs. The detached corn kernels are subsequently filtered through a grid of concave plate screens. At the same time, residual components such as cob cores and bracts are expelled via an outlet at the end of the threshing drum, thereby completing the threshing process.

The Design of Key Components

The design of the threshing drum

This paper designs a threshing drum of "variable-height threshing elements and conical roller body." The diameter of the addendum circle of the teeth at any cross-section of the threshing cylinder is a fixed value. The threshing components within the threshing cylinder combine arc-shaped plate teeth and round-headed nail teeth. The threshing drum is divided into four working zones based on its main functions: feeding, threshing, separation, and impurity discharge (Meizhou *et al.*, 2020), as shown in Figure 2.

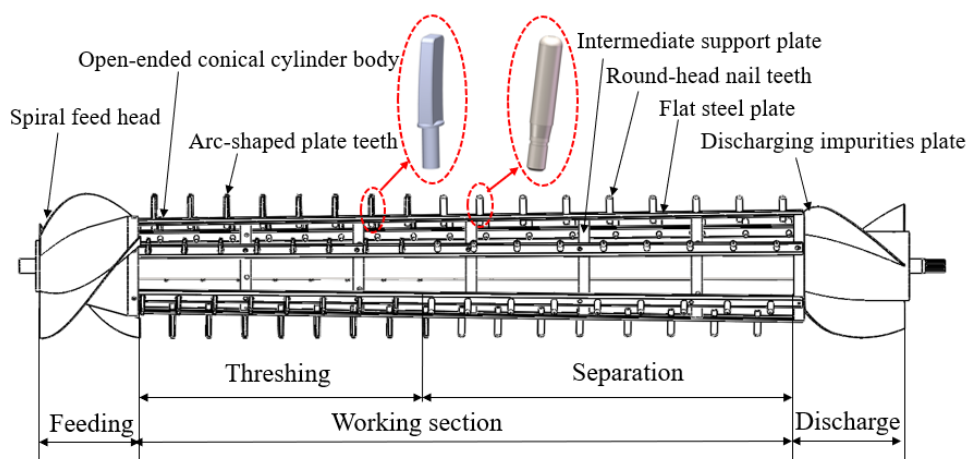


Fig. 2 - Structure diagram of threshing cylinder

Previous studies discovered that blockages mainly occurred in the first half of the threshing drum under significant feed rates. This paper employs a conical cylinder body to enhance the corn ears' accommodating capacity in the threshing cylinder's front half. Meanwhile, considering the relatively poor threshing effect at the front end of the conical cylinder body, longer threshing elements are installed at the small end of the conical cylinder body to improve the threshing capability at the front end of the conical cylinder body.

Most threshing and separation occur in the threshing section of the cylinder (Miu *et al.*, 2008). Rigid threshing at this stage can cause a significant amount of breakage. Arc-shaped plate teeth let the cobs thresh under an oblique pushing force. This threshing action is conducive to reducing grain breakage. Round-headed nail teeth feature high efficiency, a high threshing cleanliness rate, and reduced losses due to the top gnawing of grains. When applied in the separation section of the threshing cylinder, they can guarantee the threshing cleanliness rate of the device under conditions of significant feed rates (Zheng *et al.*, 2022). Meanwhile, the threshing section is designed to constitute 40% of the length of the working section, while the separating section makes up 60%. The threshing elements adopt a variable pitch arrangement that is dense at the front and sparse at the rear. In this paper, the spacing between the arc-shaped plate teeth is designed to be 138 mm, and the spacing between the round-headed nail teeth is 165 mm. The included angle between the flat steel and the axis of the roller is 30°. The distribution of the arc-shaped plate teeth and round-headed nail teeth is shown in Figure 3.

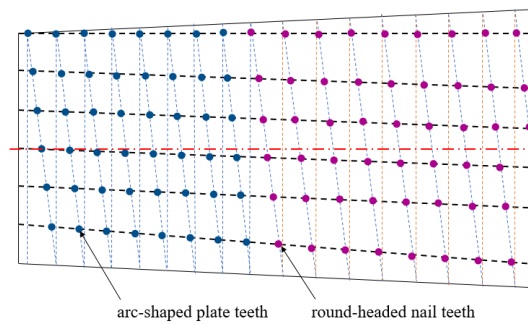


Fig. 3 - Schematic diagram of the arrangement of threshing elements on the threshing drum

The relationship between the length of the longitudinal axial flow threshing drum and the feed quantity is:

$$L = \frac{q}{q_0} \tag{1}$$

where: L denotes the working section length of the threshing drum, (m);

q represents the feeding amount of the threshing device, (kg/s);

q_0 represents the allowable feed rate per unit length in the threshing device, kg/(s·m). According to the recommendation in the "Agricultural Machinery Design Manual," q_0 is generally 3 to 4 kg/(s·m).

The unit is designed for a feed rate of 14~18 kg/s. Based on the calculation using formula (1), the value range of the unilateral threshing drum L is between 1.75 and 3.0 meters. Hence, the drum working section is designed to be 2.5 meters long.

The relationship between the diameter of the top circle of the threshing drum teeth D , the rotational speed n of the drum, and the linear speed v is as follows:

$$D = \frac{60v}{\pi n} \tag{2}$$

where: D is the diameter of the toothed top circle of the threshing drum, (m);

v is the threshing speed of the cylindrical axial roller, (m/s);

n is the rotational speed of the threshing drum, (r/min).

According to the recommendations in the "Agricultural Machinery Design Manual", the threshing speed of the cylindrical axial-flow drum (v) is 10 to 12 m/s and the threshing cylinder speed (n) ranging from 300 to 450 r/min, when substituted into Equation (2), the range of the top circle diameter of the threshing drum teeth is obtained as 430 to 760 mm. Hence, the design's top circle diameter D of the threshing drum is 550 mm. The threshing drum is a "constant-diameter drum," thus D is a fixed value.

The design of arc-shaped plate teeth and round-headed nail teeth

The corn cobs struck by the arc-shaped plate teeth will complete threshing under the continuously increasing squeezing and rubbing force, which is conducive to detaching corn kernels with different threshing difficulties. To guarantee the threshing cleanliness rate of the device, the round-headed spike teeth are designed to be arranged in the second half of the threshing drum. The structure of the arc-shaped plate teeth and the round-headed spike teeth is shown in Figure 4.

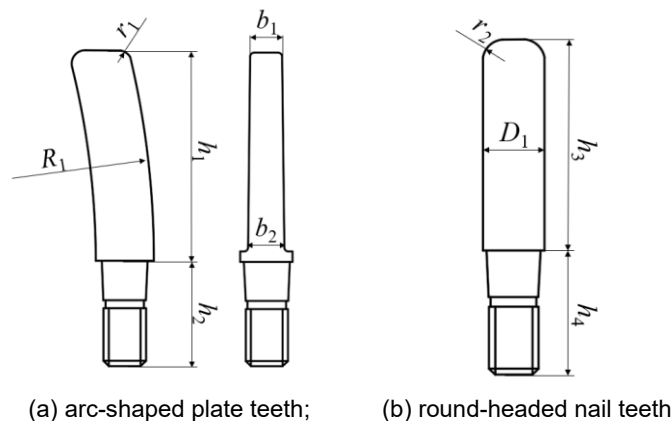


Fig. 4 - Threshing components structure

In Figure 4(a), h_1 is the working height of the arc-shaped plate teeth, taken as 75 to 95 mm; h_2 is the installation height; R_1 is the curve radius of the working surface of the arc-shaped plate teeth, taken as 344 mm; r_1 is the top fillet radius of the arc-shaped plate teeth, taken as 5 mm. b_1 is the top thickness of the arc-shaped plate teeth, taken as 12 mm; b_2 is the bottom thickness of the arc-shaped plate teeth, taken as 14 mm. In Figure 4(b), h_3 is the working height of the round-headed spike teeth, taken as 55 to 74 mm; h_4 is the installation height of the round-headed spike teeth; D_1 is the diameter of the round-headed spike teeth, taken as 20 mm; r_2 is the top fillet radius of the round-headed spike teeth. According to the theoretical research on the collision between the spike teeth and the corn cobs (Zhe, 2018), the calculation formula for the ball head radius is $R \geq 5$ mm. Therefore, in this paper, the top fillet radius r_1 of the arc-shaped plate teeth is designed to be 5 mm, and the top fillet radius r_2 of the round-headed nail teeth is 7 mm.

The threshing of corn cobs mainly occurs while moving from the upper cover plate to the bottom of the roller. During this process, the corn cobs struck by the arc-shaped plate teeth exist in two states: in contact with the concave screen or not in contact with the concave screen, as shown in Figure 5(a) and 5(b).

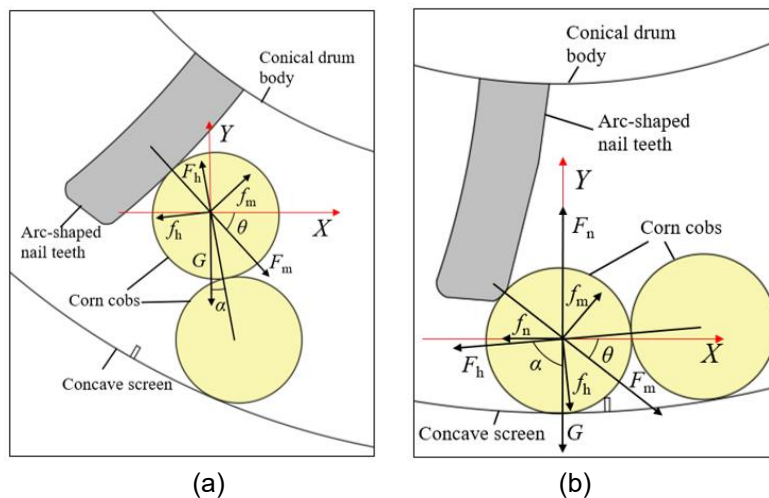


Fig. 5 - Force analysis diagram of corn cob

The force analysis of the corn cobs in these two states is carried out:

$$\begin{cases} F_{mx} = F_m \cos\theta \\ F_{my} = F_m \sin\theta \end{cases} \quad (3)$$

Figure 6(a) presents the schematic diagram of the state where the beaten ear of grain is not in contact with the concave sieve. Through the force analysis of it, the following can be obtained:

$$\begin{cases} F_x = F_{mx} + f_m \sin\theta - F_h \sin\alpha - f_h \cos\alpha \\ F_y = F_{my} - f_m \cos\theta - F_h \cos\alpha + f_h \sin\alpha + G \end{cases} \quad (4)$$

Figure 6(b) presents the schematic diagram of the contact state of the beaten ear of grain and the concave sieve. A force analysis of it yields:

$$\begin{cases} F_x = F_{mx} + f_m \sin\theta - F_h \sin\alpha - f_h \cos\alpha - f_n \\ F_y = F_{my} - f_m \cos\theta - F_h \cos\alpha + f_h \sin\alpha - F_n + G \end{cases} \quad (5)$$

where:

- F_m is the striking force of the arc-shaped nail teeth on the corn cob, (N);
- f_m - the friction force exerted on the corn cob by the arc-shaped nail teeth, (N);
- F_n - the supporting force of the concave plate screens on the corn cob, (N);
- f_n - the friction force of the concave plate screens on the corn cob, (N);
- F_h - the supporting force between the corn cobs, (N);
- f_h - the friction force between the corn cobs, (N);
- G - the gravity of the corn cob, (N);
- θ ($0^\circ < \theta < 90^\circ$) - the angle between the striking force of the arc-shaped nail teeth on the corn cob and the X-axis, ($^\circ$);
- α ($0^\circ < \alpha < 90^\circ$) - the angle between the supporting force between the corn cobs and the Y-axis, ($^\circ$).

When the corn cobs move from the upper cover plate to the bottom of the roller, affected by the impact force of the arc-shaped plate teeth and the gravity of the corn cobs, the relative position of the corn cobs and the threshing elements changes. During this process, θ gradually increases. As shown in Equation (3), the component force F_{mx} of the impact force of the arc-shaped plate teeth in the X-axis direction keeps decreasing, which slows down the axial movement speed of the corn cobs and enhances the rubbing contact between the corn cobs. At the same time, the component force F_{my} of the arc-shaped plate teeth in the Y-axis direction keeps increasing; that is, the downward pressure given by the arc-shaped nail teeth to the corn cobs gradually strengthens.

It can be inferred from Figure 5(a) and Equation (4) that to maintain the force equilibrium in the Y direction, F_h will constantly intensify, leading to a continuous increase in f_h . Combining Figure 5(b) and Equation (5), it is evident that F_h gradually strengthens, and consequently, f_h gradually rises. This rubbing and threshing process is gentle. Meanwhile, the arc-shaped plate teeth gradually squeeze the movable space of the corn cob. In this threshing process, the damage to the kernels is minor.

Design of conical drum body

The front end of the conical drum body has a smaller diameter, which enhances the grain accommodation capacity of the threshing device and strengthens the flexible contact among the corn cobs (Zhendong *et al.*, 2021). The threshing drum adopts an open type. The contact area between the open drum and the corn cobs is small, and the drum load is low, which is conducive to avoiding the problem of drum blockage caused by excessive feeding.

In this paper, the variation range of the working height of the threshing elements is designed to be 55 ~ 95 mm. As the length L of the threshing and separating section of the variable diameter open roller is 2.5 m, the taper β of the variable diameter roller body is:

$$\tan\beta = \frac{h}{L} \quad (6)$$

Hence, the taper of the conical drum body is 0.9° . This taper increases the gap at the feeding inlet by one layer of the thickness of the corn cobs compared to that at the discharge outlet, which is beneficial for smooth feeding and increasing the number of collisions between the corn cobs.

The design of the grid concave plate screens and the design of the adjustable upper cover plate with guide vanes

To prevent the uneven flow of corn cobs between the two threshing drums on both sides and influence the threshing effect, the threshing spaces of the two drums are not interconnected. Currently, the commonly used forms of concave plates include grid screens and punched screens. Grid screens have greater strength, and both the sieve porosity and separation efficiency are higher than those of punched screens. They are widely applied in existing combined harvesters. Therefore, this device employs a grid of concave plate screens. The double longitudinal axial flow grid concave plate screen is shown in Figure 6(a).

Adjusting the angle of the guide plate can control the axial movement speed of corn cobs and the material layer's thickness, significantly influencing the threshing effect. A combination guide plate with a fixed front section and an adjustable rear section is designed in the upper cover plate of the double longitudinal axial flow threshing cylinder. In this paper, the helix angle of the fixed guide plate is designed to be 24° . The helix angle range of the adjustable guide plate is designed to be 16° to 26° (Chen *et al.*, 2022). The structure of the unilateral upper cover plate is shown in Figure 6(b).

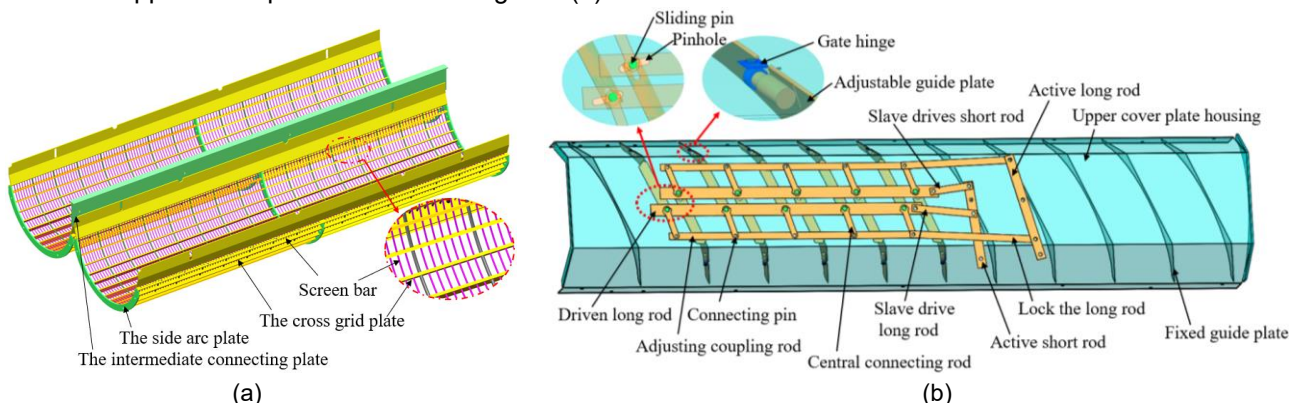


Fig. 6 - The Structural Diagram of the grid concave plate screens and the upper cover plate

One end of the adjustable guide plate is connected to the upper cover plate housing through a gate hinge, and the other end is connected to the driven long rod through a sliding pin. The other end of this driven long rod is connected to the active short rod. When the active short rod and the active long rod move simultaneously through force transmission, they cause a positional offset at one end of the adjustable guide plate. As a result, the angle of the adjustable guide plate changes, thereby controlling the axial movement speed of the corn cobs.

Experiment design

The existing research results (Chenlong *et al.*, 2022; Shulun *et al.*, 2024) indicate that the influences of the feed rate, the threshing cylinder speed, and the angle of the guide plate on the grain breakage rate are more significant than that of the threshing clearance. Hence, the feed rate, the threshing cylinder speed, and the angle of the guide plate were selected to research the device's threshing performance.

Test materials and conditions

In October 2024, a bench test was conducted at Shandong Tiankaizhongrui Machinery Technology Company Limited. The double longitudinal axial flow threshing roller was placed at an inclination of 7° to the ground, and the threshing clearance was 35 mm. The corn variety used in the experiment was "Liyuan296". The average moisture content of corn kernels was 31.3% using the LDS-1G model grain moisture detector. Thirty corn ears were taken for the physical characteristic experiments of the ears. The experimental data are as follows: the average ear length is 16.4 cm, the diameters at the middle and large ends are 49.7 mm, and the diameter at the small end is 46.9 mm. The test site is shown in Figure 7.



Fig. 7 - Testbed for double longitudinal axial flow with a large feeding amount

The threshing test of the corn threshing device

This paper conducts the corn threshing test by referring to GB/T 21961-2008 and GB/T 5982-2005. A platform scale weighs the corn cobs of the required weight and then spreads on the measurement area of the conveying device. After each test, the corn kernels in the receiving device are collected and thoroughly mixed for manual sampling, with each sample no less than 2 kg. The grain breakage rate Y_1 and the unthreshed grain rate Y_2 are calculated, and the calculation formulas are as follows:

$$Y_1 = \frac{m_s}{m_i} \times 100\% \quad (7)$$

$$Y_2 = \frac{m_j}{m_z} \times 100\% \quad (8)$$

where: m_s refers to the mass of broken grains in the sample, (g);

m_i is the total mass of grains in the sample, (g);

m_j represents the mass of unthreshed grains, (g);

m_z is the total mass of threshed grains, (g).

Single-factor test

The feed rate has a direct connection with the thickness of the material layer and thereby influences the threshing effect. The feeding quantities in this paper are set at levels 14 kg/s, 15 kg/s, 16 kg/s, 17 kg/s, and 18 kg/s respectively. The threshing cylinder speed is directly related to the striking force of the threshing components. Comprehensively considered, 300 r/min, 350 r/min, 400 r/min, 450 r/min, 500 r/min, 600 r/min, and 700 r/min were selected in this paper. The range of deflector angle adjustment for this device is 16 - 26°, and the deflector angles are horizontally set at 16°, 18°, 20°, 22°, 24° and 26° respectively.

Orthogonal test

According to the results of the single-factor experiments, the ranges of values for the test factors in the orthogonal experiments were determined. A quadratic orthogonal rotational combination experiment was carried out with three factors and levels. The three-factor level coding is presented in Table 1.

Table 1

Factors and levels of experiment			
Level	Experimental factor		
	Feed rate X_1 /(kg/s)	Threshing cylinder speed X_2 (r/min)	The angle of the guide plate X_3 / (°)
-1	15	350	22
0	16	400	24
1	17	450	26

RESULTS AND DISCUSSION

Bench tests were conducted under the experimental conditions set in this study. It was found that the unthreshed grain rate in each group was less than 0.3%, indicating a low level and demonstrating that the device performs well in terms of threshing cleanliness under these conditions. Therefore, the focus will subsequently shift to evaluating the corn grain breakage rate to further assess the threshing impact of the device.

The Results and Analysis of Single-Factor Experiment

The fixed values of the test parameters selected in this research are, respectively, the feed rate at 16 kg/s, the threshing cylinder speed at 400 r/min, and the angle of the guide plate at 16°. When carrying out the single-factor test of a certain factor, the parameters of the other two factors are selected as the fixed values. The experimental results are presented in Figure 8.

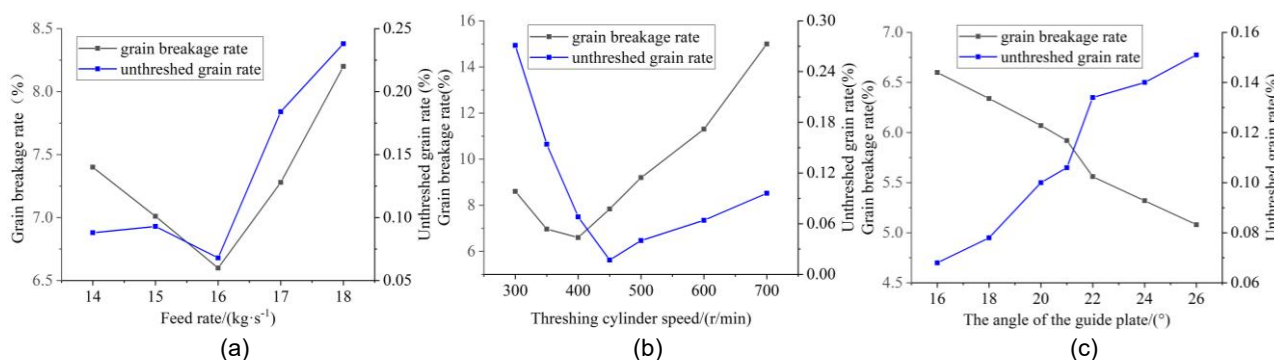


Fig. 8 - Diagram of the Results of the Single-Factor Experiment

In Figure 8(a) it is shown that with the increase in the feed rate, both the grain breakage rate and the unthreshed grain rate exhibit a trend of initially decreasing and then increasing. The reasons for this phenomenon are as follows: when the feed rate is relatively low, the corn cob being struck directly impacts the concave plate for rigid threshing, resulting in a higher grain breakage rate. Simultaneously, the axial movement speed increases rapidly upon impact due to less resistance. The threshing time is reduced, leading to a higher unthreshed grain rate. When the feed rate is relatively big, the material layer inside the roller is thicker. The threshed grains cannot be discharged from the machine in time, causing excessive impact. At the same time, it causes some corn cob to move to the impurity discharge section before the threshing is completed, resulting in a higher unthreshed grain rate.

In Figure 8(b) it is shown that as the threshing cylinder speed increases, both the grain breakage rate and the unthreshed grain rate demonstrate a trend of initially decreasing and then increasing. This is because when the threshing cylinder speed is low, the threshing time of the corn ears increases, and the number of strikes they receive increases, leading to a higher grain breakage rate. Meanwhile, the impact force of the threshing elements is small, causing some corn ears to be discharged from the machine before they are completely threshed, resulting in a higher unthreshed grain rate. At higher threshing cylinder speed, the threshing element strikes with high force, which results in higher kernel breakage and a rapid increase in the grain breakage rate. At the same time, it leads to a more incredible axial movement speed of the corn ears, causing some corn ears to be discharged from the machine before being completely threshed, resulting in a higher unthreshed grain rate.

It could be observed from Figure 8(c) that with the increase of the angle of the guide plate, the grain breakage rate shows a downward trend, while the unthreshed grain rate shows an upward trend. As the angle of the guide plate increases, the axial movement speed of the corn ears increases, which is conducive to the prompt discharge of the detached grains and avoids excessive impact, resulting in less grain crushing. Simultaneously, this behavior increases the probability of some corn ears being discharged from the machine before they are completely threshed, thereby increasing the unthreshed grain rate.

The Results and Analysis of the Orthogonal Experiment

Test Results and Analysis

The experimental scheme was designed based on the Box-Behnken module in the Design-Expert 13.0 software. With the grain breakage rate and the uncleaned grain rate as the experimental indicators, 17 experiments were carried out. The experimental scheme and results are presented in Table 2.

Table 2

Testing plan and results						
Experimental Number	Experimental Factors and Levels			Performance indicators		
	X_1 /(kg/s)	X_2 (r/min)	X_3 (°)	Y_1 %	Y_2 %	
1	16	350	22	6.21	0.252	
2	17	400	22	6.29	0.224	
3	16	400	24	5.41	0.143	
4	15	450	24	8.58	0.087	
5	15	350	24	7.49	0.274	
6	17	450	24	7.01	0.126	
7	16	400	24	5.32	0.194	
8	15	400	26	5.93	0.181	
9	16	400	24	5.62	0.092	
10	17	400	26	5.56	0.256	
11	16	400	24	5.23	0.154	
12	16	350	26	5.85	0.286	
13	16	450	26	6.73	0.046	
14	15	400	22	6.34	0.134	
15	16	400	24	5.54	0.178	
16	16	450	22	7.18	0.024	
17	17	350	24	7.72	0.246	

The data in Table 2 was analyzed for variance, and the results are presented in Table 3.

Table 3

Analysis of variance					
Source	df	Grain breakage rate Y_1		Unthreshed grain rate Y_2	
		F Value	P-value	F Value	P-value
Model	9	22.84	0.0002**	5.61	0.0166*
X_1	1	5.53	0.0510	2.19	0.1827
X_2	1	8.88	0.0205*	42.40	0.0003**
X_3	1	6.79	0.0351*	1.29	0.2940
$X_1 X_2$	1	11.57	0.0114*	0.63	0.4521
$X_1 X_3$	1	0.37	0.5644	0.032	0.8636
$X_2 X_3$	1	0.029	0.8698	0.020	0.8906
X_1^2	1	49.45	0.0002**	3.60	0.0997
X_2^2	1	112.76	<0.0001**	0.15	0.7132
X_3^2	1	5.44	0.0524	0.14	0.7202
Residual	7				
Lack of fit	3	5.17	0.0733	1.37	0.3735
Pure error	4				
Total error	16				

Note: *significant ($P < 0.05$), **very significant ($P < 0.01$)

It can be observed from Table 3 that X_1^2 and X_2^2 have an extremely significant effect on Y_1 ($P < 0.01$). X_2 , X_3 , and $X_1 X_2$ significantly influence Y_1 ($P < 0.05$). Other factors influencing Y_1 were insignificant ($P > 0.1$). Meanwhile, X_2 has an extremely significant influence on Y_2 ($P < 0.01$). Other factors influencing Y_2 are insignificant ($P > 0.1$). The $P < 0.05$ of the established regression model indicates that the relationship between the dependent variable of the regression model and the full set of independent variables is significant.

The P value of the lack-of-fit term is greater than 0.05, suggesting that the lack-of-fit is not significant, and the regression model fits the experimental results relatively well. Thus, the regression equation for the influence of each factor on Y_1 and Y_2 is obtained:

$$Y_1 = 5.97 - 0.22X_1 + 0.27X_2 - 0.66X_3 - 0.35X_1X_2 - 0.14X_1X_3 + 0.02X_2X_3 + 0.94X_1^2 + 1.27X_2^2 - 0.44X_3^2 \quad (9)$$

$$Y_2 = 0.11 + 0.019X_1 - 0.085X_2 + 0.04X_3 + 0.025X_1X_2 - 0.004X_1X_3 - 0.026X_2X_3 + 0.037X_1^2 - 0.016X_2^2 + 0.032X_3^2 \quad (10)$$

Response Surface Analysis

Through the data processing in the Model Graphs of the Analysis module, the interactive influences and influence rules of X_1 , X_2 , X_3 on the grain breakage rate are investigated. It can be known from Table 3 that the interaction effects of the three experimental factors on the unthreshed grain rate are not significant ($P > 0.05$). Thus, no further analysis is considered. The response surface results are presented in Figure 9.

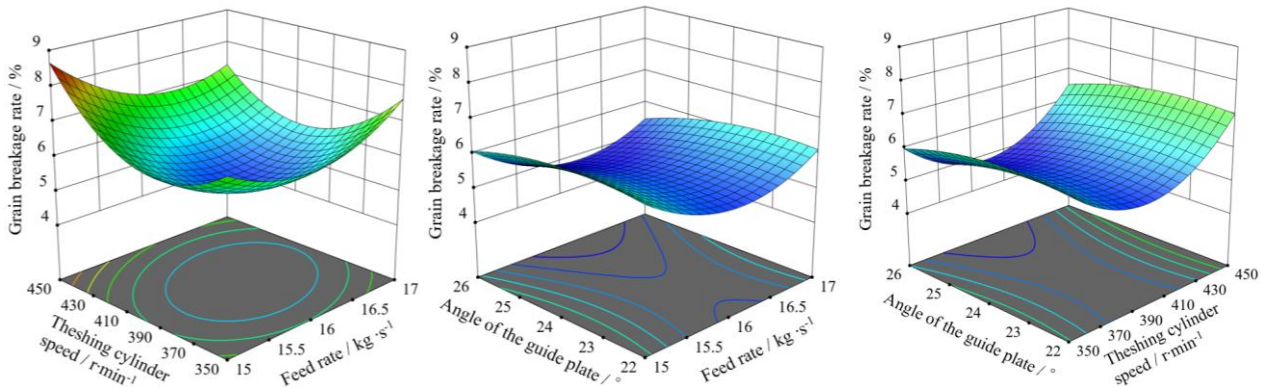


Fig. 9 - Response surface diagram of interaction factors

With the increase of the feed rate and the threshing cylinder speed, the grain breakage rate exhibits a trend of initially decreasing and then increasing, and the interaction effect of the two factors is significant. With the increase of the angle of the guide plate, the grain breakage rate shows a downward trend, while the interaction effect between the angle of the deflector plate and other factors is insignificant. This is because when both the feed rate and the threshing cylinder speed are at relatively low levels, the material layer of the corn ears is thin, and the axial movement speed of the corn ears is small. This circumstance results in, on the one hand, the impacted ears of grain directly hitting the concave screen for rigid threshing and, on the other hand, prolonging the threshing time of the ears of grain, leading to an increased breakage rate. When the feed rate and the threshing cylinder are both at relatively high levels, an overly thick material layer will impede the discharge of the detached corn kernels from the machine. Meanwhile, the excessive impact force endured by the corn ears causes the struck corn kernels to be directly crushed. Enlarging the angle of the guide plate enhances the materials' axial movement speed and reduces the material layer's thickness. This condition is conducive to the timely discharge of the already threshed corn kernels outside the machine, lowering the probability of excessive impact.

The Optimization of Threshing Parameters

The threshing effect was satisfactory. Hence, this paper's lowest grain breakage rate was taken as the optimization objective to optimize the threshing parameters. The multi-objective equation system was solved using the optimization solution module of Design Expert software. The optimal parameter combination was obtained: a feed rate of 16.057 kg/s, a threshing cylinder speed of 397.400 r/min, and an angle of the guide plate of 25.443°. The optimal parameters were simplified: a feed rate of 16 kg/s, a threshing cylinder speed of 400 r/min, and an angle of the guide plate of 26°. Multiple bench tests were carried out under this combination of parameters, and the average of the test results was taken. The actual grain breakage rate was 5.02%, and the unthreshed grain rate was 0.171%. The operational performance meets the actual harvesting requirements.

CONCLUSIONS

Existing threshing devices cannot meet the demand for large feeding volumes. This study focuses on three aspects - reducing impact force, increasing separation area, and controlling threshing time - to design a double longitudinal axial-flow corn threshing device suitable for large feeding volume conditions.

(1) Through the method of theoretical analysis, a threshing drum composed of a combined type of threshing elements of variable-height "arc-shaped plate teeth and round-head nail teeth" and a conical drum body was designed. The main structure and working process were analyzed, and the main structural parameters of the threshing drum were determined. This device satisfies the threshing requirements of high efficiency and low damage under the condition of large feed rates.

(2) The design of the arc-shaped plate teeth threshing element was based on a comprehensive analysis of the corn threshing process and mechanical considerations. It is capable of progressively increasing the squeezing and kneading force. An adjustable guide vane device was designed to control the axial movement velocity of corn cobs, thereby improving threshing performance.

(3) A large-capacity double longitudinal axial-flow threshing test rig was developed. The experiments indicate that the optimal parameter combination of this device is as follows: the feed rate is 16 kg/s, the rotational speed of the drum is 400 r/min, and the angle of the guide plate is 26°. At this point, the grain breakage rate is 5.02%, the unthreshed rate is 0.171%, and the operational performance meets the actual harvesting requirements.

ACKNOWLEDGEMENT

This work was supported financially by the Natural Science Foundation of Shandong (ZR2023ME149), the National Key R&D Program of China (2021YFD2000502), and the Opening Fund of the National Key Laboratory of Agricultural Equipment Technology (NKL2023007).

REFERENCES

- [1] Abdeen M.A., Xie G., Salem A.E., Fu J., Zhan G., (2022). Longitudinal axial flow rice thresher feeding rate monitoring based on force sensing resistors. *Scientific reports*, vol. 12, 1369, 369.
- [2] Chenlong, F., Dongxing, Z., Li, Y., Tao, C., Xiantao, H., Jiaqi, D., Huihui, Z. (2022). Power consumption and performance of a maize thresher with automatic gap control based on feed rate monitoring. *Biosystems Engineering*, vol.216, pp.147-164.
- [3] Chenlong, F., Dongxing, Z., Li, Y., Tao, C., Xiantao, H., Huihui, Z., Jiaqi, D. (2022). Development and performance evaluation of a guide vane inclination automatic control system for corn threshing unit based on feed rate monitoring. *Computers and Electronics in Agriculture*, vol.194, no.106745.
- [4] Cujbescu D., Găgeanu I., Iosif A., (2021). Mathematical modeling of ear grain separation process depending on the length of the axial flow threshing apparatus. *INMATEH-Agricultural Engineering*, vol. 65, no.3, pp.101-110.
- [5] Duanyang, G., Ke, H., Qian, W., Chengqian, J., Guohai, Z., Xiufeng, L. (2019). Design and experiment on transverse axial flow flexible threshing device for corn. Transactions of the Chinese Society of Machinery (横轴流式玉米柔性脱粒装置设计与试验). *Transactions of the Chinese Society of Machinery*, vol.50, no.3, pp.101-108; Shandong/China.
- [6] Jinliang, G., Zengjia, L., Yanfei, Z. (2024). Optimised design and simulation analysis of longitudinal flow corn cone threshing device. *INMATEH-Agricultural Engineering*, vol.73, no.2, pp.63-72.
- [7] Jiale, Z., Hainan, Z., Han, T., Xiaogeng, W., Yujun, Y. (2023). Bionic threshing component optimized based on MBD-DEM coupling simulation significantly improves corn kernel harvesting rate. *Computers and Electronics in Agriculture*, vol.212, no.108075;
- [8] Maertens K., Ramon H., Baerdemaeker J.D., (2004). An on-the-go monitoring algorithm for separation processes in combine harvesters. *Computers and Electronics in Agriculture*, vol.43, no.3, pp.197-207.
- [9] Maertens K., Babuška R., Baerdemaeker J.D., (2005). Evolutionary input selection for the non-linear identification of complex processes. *Computers and Electronics in Agriculture*, vol.49, no.3, pp.441-451.
- [10] Li, Z., Chengyu, L., Guozhen, H., Huimin, Y., Jianqun, Y., Qiang, Z. (2021). Design and experiment of bionic threshing part for high moisture content corn (高含水率玉米仿生脱粒元件设计与试验). *Journal of Chinese Agricultural Mechanization*, vol.43, no.2, pp.126-131; Jilin/China.
- [11] Meizhou, C., Guangfei, X., Chuanxu, W., Peisong, D., Yinping, Z., Guodong, N. (2020). Design and experiment of roller-type combined longitudinal axial flow flexible threshing and separating device for corn (纵轴流辊式组合玉米柔性脱粒分离装置设计与试验). *Transactions of the Chinese Society of Machinery*, vol.51, no.10, pp.123-131; Shandong/China.
- [12] Miu P.I., Kutzbach H.D. (2008). Modeling and simulation of grain threshing and separation in threshing unit—Part I. *Computers and Electronics in Agriculture*, vol. 60, no.1, pp.105-109.

- [13] Qing, T., Lan, J., Wenyi, Y., Jun, W., Gang, W. (2024). Design and experiment of high moisture corn threshing device with low damage. *INMATEH-Agricultural Engineering*, vol.74, no.3, pp.172-183.
- [14] Srison, W., Chuan-Udom, S., Saengprachatanarug, K., (2016). Effects of operating factors for an axial-flow corn shelling unit on losses and power consumption. *Agriculture and Natural resources*, vol.50, no.5, pp.421-425.
- [15] Shulun, X., Tao, C., Dongxing, Z., Li, Y., Xiaotao, H., Chuan, L., Jiaqi, D., Yeyuan, J., Wei, W., Chuankuo Z., Zhaohui D. (2024). Design and optimization for a longitudinal-flow corn ear threshing device of low loss and low energy consumption. *Computers and Electronics in Agriculture*, vol.226, no.109328.
- [16] Tao, C., Chenlong, F., Dongxing, Z., Li, Y., Yibo, L., Huihui, Z. (2019). Research progress of maize mechanized harvesting technology (玉米机械化收获技术研究进展分析). *Transactions of the Chinese Society for Agricultural Machinery*, vol.50, no.12, pp.1-13; Beijing/China.
- [17] Vlăduț N.-V., Biris, S.St., Cârdei, P., Găgeanu, I., Cujbescu, D., Ungureanu, N., Popa L.D., Perişoară, L., Matei, G., Teliban, G.-C., (2022). Contributions to the Mathematical Modeling of the Threshing and Separation Process in An Axial Flow Combine. *Agriculture*, vol. 12, no.10, 1520.
- [18] Vlăduț N.-V., Ungureanu, N., Biris, S. St., Voicea, I., Nenciu, F., Găgeanu, I., Cujbescu, D., Popa, L.-D., Boruz, S., Matei, G., Ekielski, A., Teliban, G.C., (2023). Research on the identification of some optimal threshing și separation regimes in the axial flow apparatus. *Agriculture*, vol. 13, no.4, 838.
- [19] Xiaopeng, H., Chenhe, L., Jianfang, S., Guangwan, W. (2003). Development of extruded and rolled corn sheller (挤搓式玉米脱粒机的研制). *Transactions of the Chinese Society of Agricultural Engineering*, vol.19, no.2, pp.105-108; Beijing/China.
- [20] Xinpin, L., Yidong, M., Xin, J., Lianxin, G. (2015). Design and test of corn seed bionic thresher (玉米种子仿生脱粒机设计与试验). *Transactions of the Chinese Society for Agricultural Machinery*, vol.46, no.7, pp.97-101; Henan/China.
- [21] Yujia, D., Guohai, Z., Aoqi, Z., Jitan, L., Jia, Y., Xin, W., Xiaohui, Y. (2023). Experimental analysis of threshing maize seeds with high moisture content. *INMATEH-Agricultural Engineering*, vol.69, no.1, pp.131-144.
- [22] Yuejiang, T., Chengqian, J., Yanpu, C., Peng, L., Xiang, Y., Enting, W., Kang, Y. (2020). Design and optimization of segmented threshing device of combine harvester for rice and wheat. *Transactions of the Chinese Society of Agricultural Engineering*, vol.36, no.12, pp.1-12; Shandong/China.
- [23] Youliang, N., Chengqian, J., Tingen, W., Lei, Z., Zheng, L. (2022). Design and experiments of the 4LZ-1.5 soybean combine harvester (4LZ-1.5 型大豆联合收获机设计与试验). *Transactions of the Chinese Society of Agricultural Engineering*, vol.38, no.22, pp.1-11; Nanjing/China.
- [24] Zheng, Z., Hongmei, Z., Mingtao, H., Hao, H., Liquan, Y., Wanzhang, W. (2022). Design and experiment on corn thresher with tangential-axial flow double-roller (切轴流双滚筒玉米脱粒试验台设计与试验). *Journal of Chinese Agricultural Mechanization*, vol.44, no.6, pp.45-52; Henan/China.
- [25] Zhe, Q. (2018). Research on combined maize threshing and separating device with low damage. PhD Thesis, China Agricultural University, Beijing/China.
- [26] Zhendong, W., Tao, C., Dongxing, Z., Li, Y., Xiantao, H., Zepeng, Z. (2021). Design and experiment of low damage corn threshing drum with gradually changing diameter (玉米收获机低损变径脱粒滚筒设计与试验). *Transactions of the Chinese Society of Machinery*, vol.52, no.8, pp.98-105; Beijing/China.
- [27] ***China Statistical Yearbook 2024, *Agriculture*, Available from: <https://www.stats.gov.cn/sj/ndsj/2024/indexch.htm>